



# Seismic site characterization using multichannel analysis of surface waves in the Singhbhum region of Jharkhand, India: a case study

Ashhad Imam<sup>1</sup> · Keshav K. Sharma<sup>1</sup> · Virendra Kumar<sup>1</sup>

Received: 28 September 2022 / Accepted: 12 March 2023 / Published online: 1 April 2023  
© Akadémiai Kiadó 2023

## Abstract

The present study carries out subsurface exploration of Jamshedpur region using Active Multichannel Analysis of Surface Waves techniques that provide information on the different lithological characteristics. Four different sites (MASW-1 to MASW-4) were chosen in proximity to river basin to obtain a probable shear wave velocity profile. To record the raw wave field traces produced by a 10 kg sledgehammer, a linear array of 24 numbers of 4.5 Hz geophones was employed. The effects of data acquisition parameters, like sampling frequency (500 Hz, 1000 Hz, and 2000 Hz) and offset distance (1 m, 6 m, 8 m, and 20 m), were used to obtain a high-resolution dispersion image. Due to the variables selected as data acquisition parameters, the optimal set of data parameters was found, providing the best resolution of dispersion images for all the selected sites. The results indicate that the best resolution of the dispersion image was produced at an offset distance range of 6–8 m at sampling frequencies range of 500–1000 Hz at 1 m geophone spacing with five stacking, indicating a strong signal to noise ratio in a range of 80–90%. Up to a depth of ~3 m, stiff silty clay soil was discovered, and at depths of 30 m or more, medium- to very-dense weathered mica schist was discovered. At sites MASW-1 and MASW-3, respectively, slag fillings were found in the top layer at depths of 1.2 and 2.3 m. Greater depths of hard rock layers have also been found at site MASW-3. Locations along the river generally fall into National Earthquake Hazards Reduction Program (NEHRP) categories C or D.

**Keywords** Multichannel analysis of surface waves · Shear wave velocity · Site classification · Dispersion image · Inversion analysis

---

✉ Ashhad Imam  
ashhad.ce@gmail.com

Keshav K. Sharma  
kksharma.ce@nitjstr.ac.in

Virendra Kumar  
kumarvirendra57@gmail.com

<sup>1</sup> Department of Civil Engineering, National Institute of Technology Jamshedpur, Jamshedpur 831014, India

## 1 Introduction

When attempting to ascertain how earthquake shaking presents itself on the ground's surface, it is crucial to take the velocity characteristics at a shallow level into account. The shear wave velocity, represented by  $V_s$ , is a crucial quantity for figuring out the dynamic characteristics of the soil in the shallow subsurface. Studies of the generation and propagation of seismic waves are frequently employed in earthquake geotechnical engineering. Geophysical exploration has come a long way since the advent of surface wave technologies for the purpose of detecting the soil subsurface profile. Using a range of geophysical techniques, the near-surface has been detailed and the shear wave velocity has been measured. Spectral Analysis of Surface Waves (SASW) and Multichannel Analysis of Surface Waves (MASW) are the techniques that are employed most commonly. These geophysical methods employ a wide range of processing methods, testing settings, and inversion algorithms (Haloi and Sil 2015; Kramer 1996).

$V_s$  is a dynamic soil property that has been connected to several other soil properties, including shear modulus, bulk modulus, fundamental vibration frequency, seismic amplification, and Poisson's ratio (Dikmen et al. 2010). Important geotechnical and earthquake engineering applications of  $V_s$  include the assessment of soil liquefaction potential, characterization of seismic sites, assessment of seismic site effects, and study on seismic micro zonation (Ashraf et al. 2018; Salas-Romero et al. 2021; Eker et al. 2012; Trupti et al. 2012; Field and Jacob 1993; Kwok et al. 2008; Rathje et al. 2010; Stewart et al. 2014; Anbazhagan and Sitharam 2008; Borchardt 1994). One of the most crucial things to consider when assessing the degree of seismic risk posed by each place is whether or not there is considerable ground motion. Given that the properties of the top 30 m subsurface profile have a significant impact on seismic ground motions, the parameters determined in the upper 30 m provide us with important information in respect to site response studies (Anderson et al. 1996). Using the  $V_{s,30}$  estimate, it is possible to anticipate future site amplification and de-amplification (Anbazhagan and Sitharam 2008; Dobry et al. 2000).

Despite the fact that other surface wave techniques have been evolved, the multi-channel analysis of surface waves (MASW) approach has most recently gotten positive reviews (Park et al. 1999, 2007). A  $V_s$  profile for the area under inquiry can be produced with the aid of the non-destructive seismic studies technique known as MASW (Salas-Romero et al. 2021). The advantages of the MASW technique include testing the ground in its natural state, averaging non-uniformity, being economical and environmentally friendly, and completely expressing the complex nature of seismic waves, volume, and lateral continuity in the survey. Using geophysical tools, one can effectively investigate the spatial variability of a site's underlying properties. The primary benefits of each technique are that it is non-intrusive and non-destructive, and the evaluation process is completed in a relatively short amount of time (Adegbola et al. 2013; Pegah and Liu 2016; Socco and Strobbia 2004; Socco et al. 2010; Foti et al. 2018). Despite the benefits of the MASW approach, a number of issues need to be resolved in order to ensure the accuracy of the data gathered. One of the main issues is the accuracy of the calculated  $V_s$  profile. The accuracy in  $V_s$  not only depends on the variability in the estimated phase velocity (that is, dispersion curves) but also depends on the uncertainties introduced in the inversion procedure (for instance, the solution non-uniqueness). The process of assessing the accuracy of the  $V_s$  profile is drawing the variance curve during data analysis. The following data analysis used the most accurate dispersion curve analysis

possible thanks to ideal acquisition conditions (Park et al. 1999). It is essential to ensure that a high-resolution dispersion image is captured during data acquisition due to the impact on the plot of the dispersion curve.

An additional essential component of the investigation was the resolution of the dispersion images that were produced by the Active MASW survey. It is shown that modifying the field geometry in conjunction with other variables yields dispersion images with varying resolutions (Park et al. 1998). The objective was to locate the best possible dispersion images so that an appropriate extraction of the dispersion curve revealing the fundamental mode could be accomplished (with a good signal-to-noise ratio). This curve can then be utilized in an inversion technique to predict the subsurface stiffness profile with the highest probability (Ariffin et al. 2016; Thitimakorn 2013; Madun 2016). To obtain the correct shear wave velocity profile, it is necessary to extract an accurate dispersion curve which indicates high signal-to-noise ratio (SNR). In addition, if the resolution of the resulting dispersion image was not high enough, the process of retrieving the information would be more challenging. Determining the effect of several data acquisition parameters on image resolution is therefore a key component of the study. Several studies in relation to effects of several data acquisition parameters are reported in the literature (Basri et al. 2020; Park et al. 1999, 2002, 2001; Gosar et al. 2008; Park 2011; Dikmen et al. 2010; Louie 2001; Grandjean and Bitri 2006; Socco et al. 2009, 2010). The resolution of the dispersion image can be affected by a variety of factors, including the sampling frequency, the offset distance, the inter-receiver spacing, and the total number of channels, the kind of source energy, the striker or the base plate, as well as other data acquisition parameters (Xia et al. 1999; Tian et al. 2003a, b; Liu et al. 2004).

The "offset distance" also referred as the distance between the initial geophone transmitter and the source, is of the utmost importance for acquiring reliable wave field recordings and high-resolution dispersion images (Stokoe et al. 2017; Park et al. 1999). Active surveys generate both body waves and surface waves, with body waves being more prominent close to the impacting source due to the compression waves generated by the impact. Surface waves are not developed at the vicinity of source point because they are formed through interference of (*P* and *SV*) body waves generated from reflections and refractions, occurrence of which require a certain minimum distance from the source. Therefore, the first receiver closest to the source should be placed beyond this point, and this is called the near-field effects. If a receiver is placed within this distance, it will record either body or ambient noise wave fields. This minimum distance changes with wavelength a longer wavelength needs a longer distance to be fully developed. A rule of thumb is 25–50% of the wavelength (Park et al. 1999). When body waves or ambient noise wave fields are added, nonplanar waves arise. The receiver array is designed to capture planar wave fields, usually surface waves, after the generated wave field has travelled a set distance from its source. Waves with longer wavelengths travel further before becoming planar, and vice versa. Furthermore, a significant source-offset distance may cause the wave field energy to be attenuated even before it reaches the geophone array. Frequently, it is also observed that all the dominant waves are entirely not recorded by the geophone array, which is responsible for missing data in the collected record (Imam et al. 2022). When the source offset is higher than half the longest wavelength, plane-wave propagation of surface waves occurs in most circumstances (Park et al. 1999).

The far-offset effect describes the location at which the impact-generated wave field cannot be captured by the geophone array. Due to attenuation and geometrical spreading, surface waves weaken substantially over longer distances, or they become contaminated by a dominant undesired noise wave field, such as dispersed surface waves (correspond to

higher modes), random ambient noise, and road noise (Park 2011). Higher modes of surface waves, which may dominate over large distances because of their lower attenuation, can also produce contamination. As for higher-mode surface waves, the "contamination" depends on the goal of the dispersion analysis. If the inversion relies only on fundamental-mode data, they are an element of disturbance. However, higher-mode data can often provide useful information that can be tackled through a multimode inversion (Gabriels et al. 1987). Because of this, there are two unique sorts of offset effects, namely near-offset effects and far-offset effects, and a substantial amount of research has been conducted on both of these types of offset effects (Park et al. 1999, 2002; Park 2011; Sanchez-Salinerio et al. 1987; Tokimatsu 1995; Zywicki and Rix 2005; Strobbia and Foti 2006; Yoon and Rix 2009; Rahimi et al. 2021). The distribution of wavelengths across the wave field is one of the factors that help to establish the parameters of the near- and far-offset effects. In this study, the optimal offset is the range of distance away from the source that enables surface waves to be developed with the highest efficiency in order to estimate the subsurface velocity ( $V_s$ ) for a depth range of 0–30 m. The field geometry variables known as source offset ( $XI$ ) and receiver spread length ( $L$ ) are related to one another in a significant way. The best configuration of these two variables suggests, in essence, that the offset shouldn't be either too close to or too far away from the seismic source.

According to an analytical evaluation of the literature, the majority of active MASW surveys utilize a wide range of parametric configurations to fulfil the aims of the study. This is the case despite the fact that substantial research has been conducted on active MASW surveys. A few studies have been published in the literature that make an effort to offer suggestions regarding the selection of various factors in the ongoing MASW survey in order to increase the precision of estimation (Foti et al. 2018; Li and Rosenblad 2009; Yoon and Rix 2009; Rahimi et al. 2022). It has been observed that the researchers have different opinions regarding the parameters that should be utilized most effectively so that appropriate subsurface profiles could be generated. The level of detail that can be seen in the dispersion image has a significant impact on the validity of the findings. A review of the literature indicates that the best or most appropriate parameters were previously chosen for dispersion picture resolution primarily based on eye inspection and inferences.

However, it is required to give a quantification support for the resolution of the dispersion images, so that the best suited parameters may be selected. Furthermore, the precision of the derived dispersion curve affects the trustworthiness of the subsurface shear wave velocity profile. In recent years, a number of different software packages are available that are capable of automatically extracting the dispersion curve, which has led to results that are more precise, accurate, and dependable. The following is a list of the scope of work in this study:

1. Carrying out an active MASW survey at several designated locations in the proximity area of Kharkai River, Jamshedpur; this survey will include a variety of subsurface characteristics; various data acquisition parameters will also be taken into consideration.
2. Investigating different locations to figure out the optimal data acquisition parameters for each location to achieve the highest resolution dispersion image, which would then enable the precise extraction of the fundamental mode (i.e., quality signal), resulting in the generation of a shear wave velocity profile that is appropriate for the depth. Consequently, it was required to determine how changes in data acquisition parameters influenced the resolution of the dispersion images (sampling frequency and offset distance at five levels of stacking with a geophone spacing of one meter).

- To acquire the 1D and 2D shear wave velocity ( $V_s$ ) profile and then compare the result to the data from the borehole. In addition, an average shear wave velocity, denoted by the notation  $V_{s30}$ , will be computed in order to determine the site classification studies.

This paper presents the findings of a study that was carried out on the bank of kharkai river basin in Jamshedpur region of Singhbhum district with the goal of determining the  $V_{s30}$  and to estimate the prospects of possible infrastructural development in the specified region. Following the collection of field data via an active MASW survey, the "Parkseis" software was used to analyze the data and interpret the outcomes of the study.

## 2 Methodology

An Active MASW investigation that was carried out in the field is schematically depicted in Fig. 1. A linear arrangement of geophone receivers can identify seismic waves produced by the strike of sledge hammer or weight drop system, that propagate through the ground. A portable seismograph is connected to the geophone receivers along with a data acquisition system (DAQ) (as shown in Fig. 1). Field experiments are used to collect the raw wave fields, which are then subjected to preprocessing, dispersion, and inversion analyses, among other stages of analysis. Parkseis 3.0, data processing software was additionally used in this regard to interpret the unprocessed signals captured during the field investigations and produce a high-resolution dispersion image, from which an appropriate dispersion curve was extracted to obtain the shear wave velocity profile for the designated site.

ParkSeis (PS) processes Rayleigh-type seismic surface waves acquired from MASW ("multichannel analysis of surface waves") surveys. PS will generate shear-wave velocity ( $V_s$ ) profile (1-D or 2-D) by analyzing the fundamental-mode ( $M0$ ) dispersion curve of Rayleigh waves. The starting input data file should consist of one or more of raw field data sets, called "records", recorded by using a multichannel recording device; for example, a 24-channel engineering seismograph. Although the minimum number of channels for the input data tested with PS was four (4), it is highly recommended that the recording device have twelve (12) or more channels (ParkSeis User Guide).

A network of ground-based geophone receivers is used to record the vibration caused by waves that are propagating from an active impulsive source (Xia et al. 2004). The

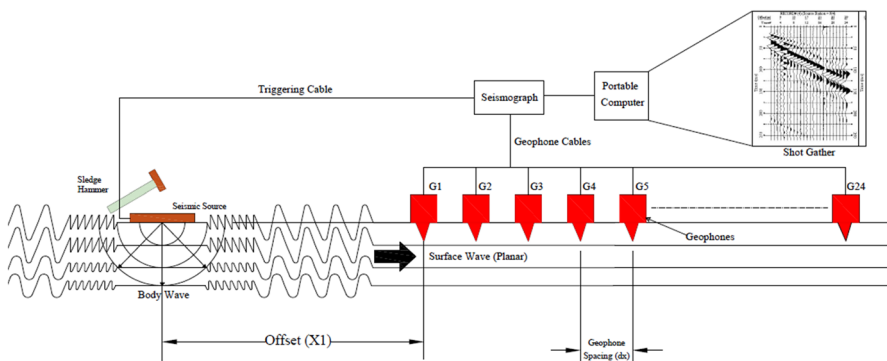


**Fig. 1** Pictorial representation of data acquisition setup in MASW

dispersion image is created by converting the time signatures to the frequency domain, and the dispersion curve is formed by demarcating combinations of phase velocities and frequencies that have the highest energies in the area (Park et al. 2001). The flowchart in Fig. 2 provides an overview of the whole process that is involved in conducting a MASW survey, regardless of whether the survey is active or passive.

Rayleigh wave dispersion curves are generated using dispersion analysis using surface wave data. The basic mode dispersion curve is extremely important when using the collection of surface wave analysis software tools that have been developed. The dispersion analysis is the process of extracting dispersion curves from a time series that has been collected. There are a variety of methods that can be employed. There are several transform-based approaches for active testing, the most common of which are the slowness–frequency ( $p$ – $\omega$ ) transform, the frequency–wave number ( $f$ – $k$ ) transform, and the phase shift method (Park et al. 1998), which are all based on the slowness–frequency transform for active type of testing (Socco et al. 2009). In the present study, phase shift method was used for carrying out dispersion analysis of the seismic field records.

## 2.1 Location details and geology of the study area

The city of Jamshedpur may be found in the southernmost part of the state of Jharkhand (its coordinates are as follows: latitude  $22^{\circ} 12' - 23^{\circ} 01' N$  and longitude  $86^{\circ} 04' - 86^{\circ} 54' E$ ). The city is located inside the East Singhbhum district, which has a remarkable geological past that sets it apart from other districts. A significant thrust zone can be found stretching from Beharagora in the southeast all the way up to the east of Jamshedpur, and it continues on into the Saraikela Kharsawan district. The shear zone divides the landscape between a northern terrain consisting of rocks that have been significantly metamorphosed and a southern terrain consisting of rocks that have been considerably less metamorphosed. The rocks that make up the ground beneath the region date from the Archean all the way up to the Tertiary era. Granites, granite-gneisses, phyllites, Mica schists, quartzites, metabasics, and basic lavas make up a significant portion of the area. In addition to being in Seismic Zone II (this location is categorized as the Low Damage Risk Zone by the Indian Standard (IS) Code, for which a zone factor assigned by IS code is 0.10), and Jamshedpur is also part of the larger Chota Nagpur Plateau. Because of variations in the lithology and rock's stiffness, seismic waves in the area will behave differently during large and major earthquakes. As a result, it is necessary to study the area in order to characterize the material that is close to the subsurface. Because of which, a case study was conducted at four

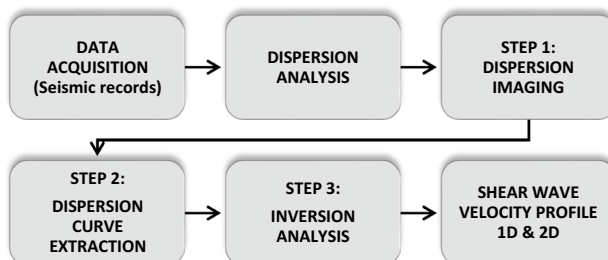


**Fig. 2** Flowchart illustrating several data collecting and processing processes in the MASW approach

locations in the city of Jamshedpur, which can be found on the bank of the Kharkai River (see Fig. 3 for more details).

### 2.2 Details of test setup

A number of experimental investigations using a variety of parameters are necessary to determine the suitable data acquisition configurations that have an effect on the accuracy

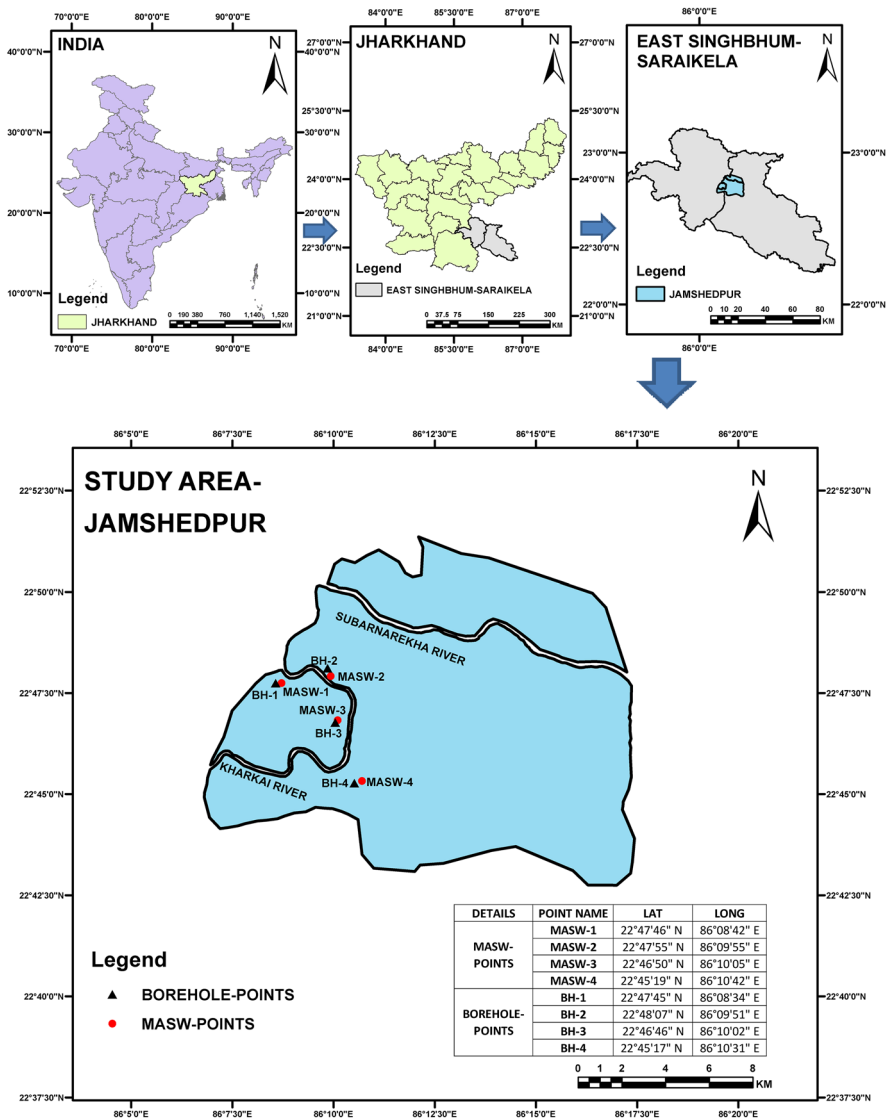


Fig. 3 Location details of study area

of the subsurface profile. In this particular investigation, a seismic event was recorded with the use of a linear array consisting of 24 channels of 4.5 Hz geophones connected to a seismograph (Dolang DBS280B V3). The surface wave propagation was generated by the impact of a 10 kg sledgehammer on the Aluminum based striker plate. On the other hand, the coupling resonant frequency for geophones is determined by the firmness of the soil. Because the firmness of the soil increases with depth, the coupling resonant frequency can be increased by burial of the geophones or by the use of longer spikes. Adequate coupling is very important in shear-wave recording because the rocking of geophones causes a low-frequency coupling resonance. Noting this, it was assured in the field, that the geophones be planted with their bases firmly contacting the soil. The current study was based on a linear active MASW survey that was carried out in the border region of the districts of East Singhbhum and Saraikela in a total of four different places (as shown in Fig. 3). Several experimental studies were performed using the different parameters presented in Table 1 to determine the optimal data acquisition parameters using the same setups.

### 3 Results and discussions

#### 3.1 Dispersion analysis

The evidence for how different data acquisition parameters of an active MASW survey affect distinctive features of the resulting dispersion images is provided in the section below. It is required to obtain a high resolution dispersion image which will be indicating a high S/N ratio so that an adequate shear wave velocity profile along the depth is obtained. The offset distance, receiver spacing, sampling frequency, stacking, etc., all affect a dispersion image's resolution (Kramer 1996; Miller et al. 1999; Xia et al. 1999). In order to get the best parameters for data gathering, taking into account the different characteristics that have previously been covered in the preceding sections, a number of active MASW experiments were conducted at the bank of the Kharkai River in this respect. The resolution of the produced dispersion image and a visual examination of the shear wave velocity profile serve as indicators of this parameter's influence. This study offers appropriate guidance for high image resolution disseminated in ongoing MASW experiments and is valuable for confirming the impact of parameters. Table 2 presents a summary of the findings for all sites.

However, to depict the influence of the parameters towards attaining good resolution of dispersion images, a typical results for one of the location (designated as MASW-4, Coordinates: 22° 45' 19" N 86° 10' 42" E) is discussed in the next section. To investigate

**Table 1** Survey parameters adopted for MASW investigation

Varying parameters	Level of variations
Source offset ( $XI$ )	1 m, 6 m, 8 m, 20 m
Sampling frequency	500 Hz, 1000 Hz, 2000 Hz
Source (Sledgehammer)	10 kg
Stacking	5 no. of shots
Receiver spacing ( $dx$ )	1 m (Fixed for all sites)
Sampling length	512 samples



**Table 2** Optimum Data Acquisition parameters obtained for all the sites chosen for Active MASW survey

Site	Coordinates	Data acquisition parameters adopted		Optimum data acquisition parameters		Average <i>S/N</i> ratio (%)
		Sampling frequency (Hz)	Offset (m)	Sampling frequency (Hz)	Offset (m)	
MASW-1	22°47'46" N 86°08'42" E	500, 1000, 2000	1, 6, 8, 12	1000	8	88
MASW-2	22°47'55" N 86°09'55" E	500, 1000, 2000	1, 6, 8, 20	1000	6	84
MASW-3	22°46'50" N 86°10'05" E	500, 1000, 2000	1, 6, 8, 20	500	8	80
MASW-4	22°45'19" N 86°10'42" E	500, 1000, 2000	1, 6, 8, 20	500	6	85

1 m geophone fixed spacing with option of five stacking (5 no. of shots) was adopted. Optimization was based on visual quality of image, *S/N* Ratio, identification of noise adulteration or over toning of dispersion image

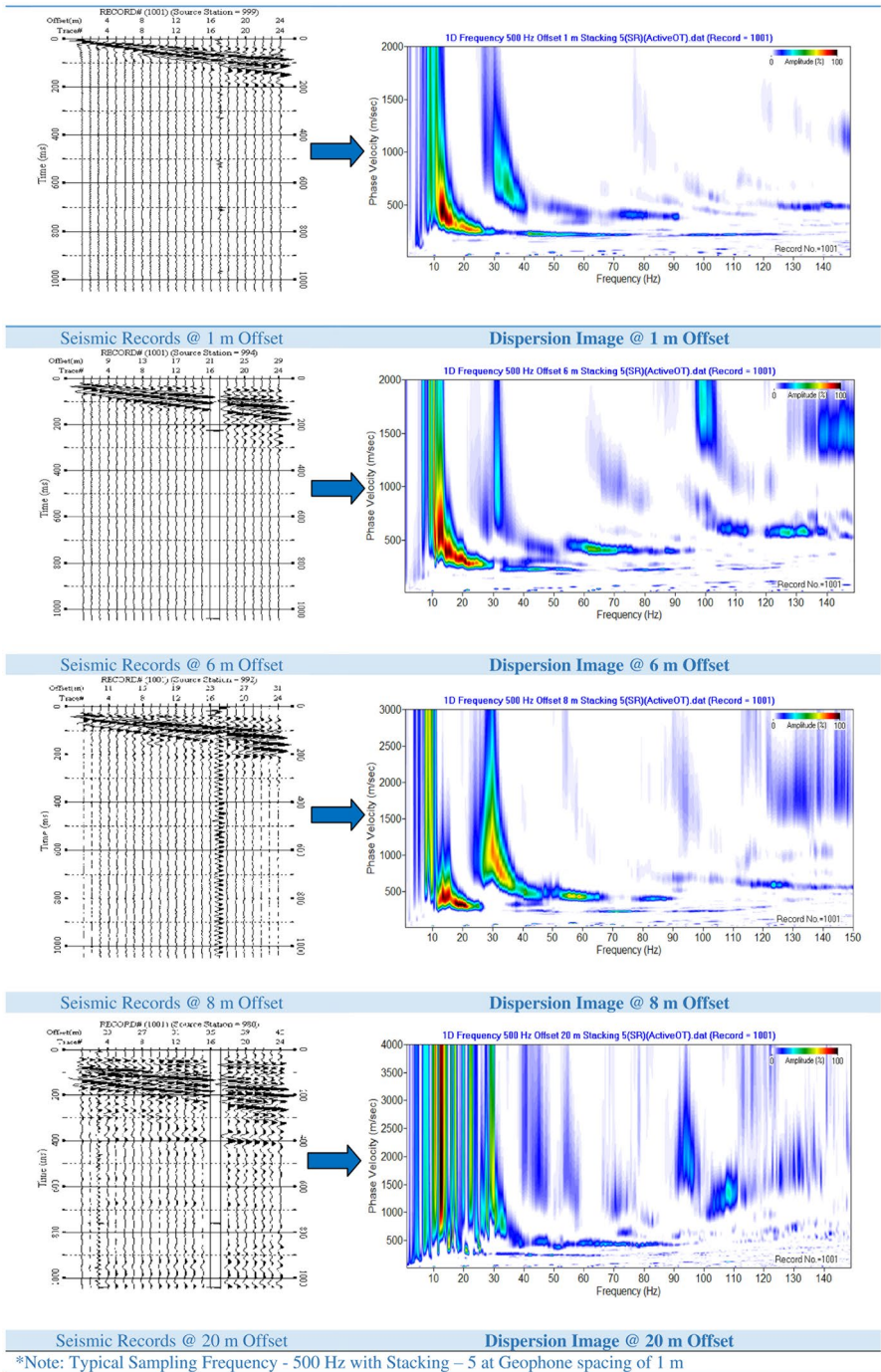
the impact of the offset distance on the resolution of the dispersion image, a linear type of spread with a spread length of 23 m and a geophone spacing of 1 m was recorded at the site location (MASW-4). In this instance, four MASW data for various offsets were acquired (1, 6, 8, and 20 m). Figure 4 displays the seismic data and generated dispersion images for various offsets.

### 3.1.1 Data acquisition parameters

The information presented in this section demonstrates how the various data collection parameters used during the active MASW survey has an effect on the observable properties of the dispersion images that are produced. This work aims to highlight the significance of these components in getting the appropriate resolution for dispersion images derived from an Active MASW survey and to provide some guidance with relation to this topic.

**3.1.1.1 Source offset: impact on the resolution of dispersion image** The dispersion images obtained for the investigations with a 1 m offset show a weak fundamental mode, with the energy content accumulating mostly in the low-frequency region (that is a slight reduction of the phase velocity at low frequencies), showing a near-offset effect, i.e., offset = 1 m (Refer Fig. 4). In the event of a 1 m offset, a slight 2<sup>nd</sup> order mode is also seen. For surveys carried out with 6 m, the trend of the fundamental mode dispersion image, however, becomes discernible and continuous, producing a dispersion image that can be seen visually. Additionally, it is discovered that the basic dispersion band formed with a 6 m offset (Fig. 4) is more defined and spans a greater frequency range, or around 11–28 Hz.

Moreover, in this situation of a 6 m offset, the higher order modes are likewise not very noticeable. However, in the dispersion image with an 8 m offset, over toning traces may be easily seen. The resulting dispersion images at 20 m offset, as shown in Fig. 4, show immense adulteration all through the frequency range of analysis. Such adulteration causes the calculated dispersion curve to have a low *SNR* because of the far offset effect. It follows that the distant offset effect causes the dispersion images to become increasingly skewed



Seismic Records @ 1 m Offset      Dispersion Image @ 1 m Offset  
Seismic Records @ 6 m Offset      Dispersion Image @ 6 m Offset  
Seismic Records @ 8 m Offset      Dispersion Image @ 8 m Offset  
Seismic Records @ 20 m Offset      Dispersion Image @ 20 m Offset  
\*Note: Typical Sampling Frequency - 500 Hz with Stacking - 5 at Geophone spacing of 1 m

**Fig. 4** Typical seismic records and corresponding dispersion images obtained for different offset distances for site MASW-4

as the offset distance rises. Large signal-to-noise ratios were found to be represented in the general spectrum by high-amplitude dispersion curves with distinct distributions across various modes and succeeding high frequencies. High amplitude and uninterrupted higher frequencies were attained with a medium length source offset distance, according to Olafsdottir et al. (2016).

The purpose of this study is to determine an appropriate offset distance in order to successfully represent substrata features using inverted profiles and generate a high-resolution dispersion image with a recognized fundamental mode exhibiting a clear *M0* dispersion curve i.e. dispersion curve representing fundamental mode. A 6 m offset with a 1 m receiver spacing is the optimal design for the site that has been selected in this particular instance. The results for the offset distance are consistent with and agree well with the suggestions made by earlier studies (Park et al. 2002; Penumada and Park 2005). The recommended values, according to some sources, can have a tolerance of 20% and need to be updated regularly depending on testing done in different places with different types of soil (Park 2011; Park et al. 2001; Imam et al. 2022). In order to get a high-resolution dispersion image from a location that has stiff strata, it is possible that an offset choice of 6–8 m will be regarded sufficient despite the fact that there are practical uncertainties.

**3.1.1.2 Sampling frequency: impact on the resolution of dispersion image** The sampling rate, also known as "samples per second," is defined as the average number of samples that are captured in each second. The frequency spectrum that is retrieved is subject to some degree of variation from the sampling rate. According to the requirements outlined by Nyquist, the sampling frequency, which is the inverse of the sampling interval, needs to be at least twice as high as the frequency of the signal that is being propagated at its strongest. For geo-engineering scale surface wave evaluation, a sampling frequency of 500 Hz and a sampling period of 2 ms are usually suitable (Foti et al. 2018).

Within the scope of this investigation, a standardized sample size of 512 samples was combined with three distinct sample frequencies (2000 Hz, 1000 Hz, and 500 Hz). The sampling interval, which is governed by the requirements of the site, is responsible for determining both the frequency and the volume of the samples that are collected. Because the wave is able to move more quickly in a stronger stratum than in a softer one, the amount of time necessary for acquisition is reduced. The MASW recordings and their dispersion images obtained for various sampling frequencies are displayed in Fig. 5 for the proposed location MASW-4. This location has a typical offset distance of 6 m, and the geophone receiver spacing is 1 m at 5 numbers of stacking.

The results are illustrated in Fig. 5 with a sample frequency of 2000 Hz. In the case of the frequency of 2000 Hz, the geophone array did not completely record all of the dominating waves; as a result, there is missing data in the record that was gathered. It seems that the sampling duration of 256 ms, was insufficient to finish the phases. On the other hand, Fig. 5 shows raw data with a sample frequency of 1000 Hz and 500 Hz, respectively. The sampling duration (ratio of total length of samples to sampling frequency) for the same is  $512/1000 = 512$  ms and  $512/500 = 1024$  ms, respectively, shows that the recording duration is just right for all the dominant phases to travel through the geophone array entirely, thereby resulting in a finer resolution of the dispersion image. However, the records with lower sampling frequencies (less than 500 Hz) may complete its dominant phases of recording the signal, but unnecessary increase in sampling time is not useful in obtaining any additional information and, in fact, is detrimental to signal quality due to unwanted noise adulteration. In such cases, the geophone continues to record ambient signals even

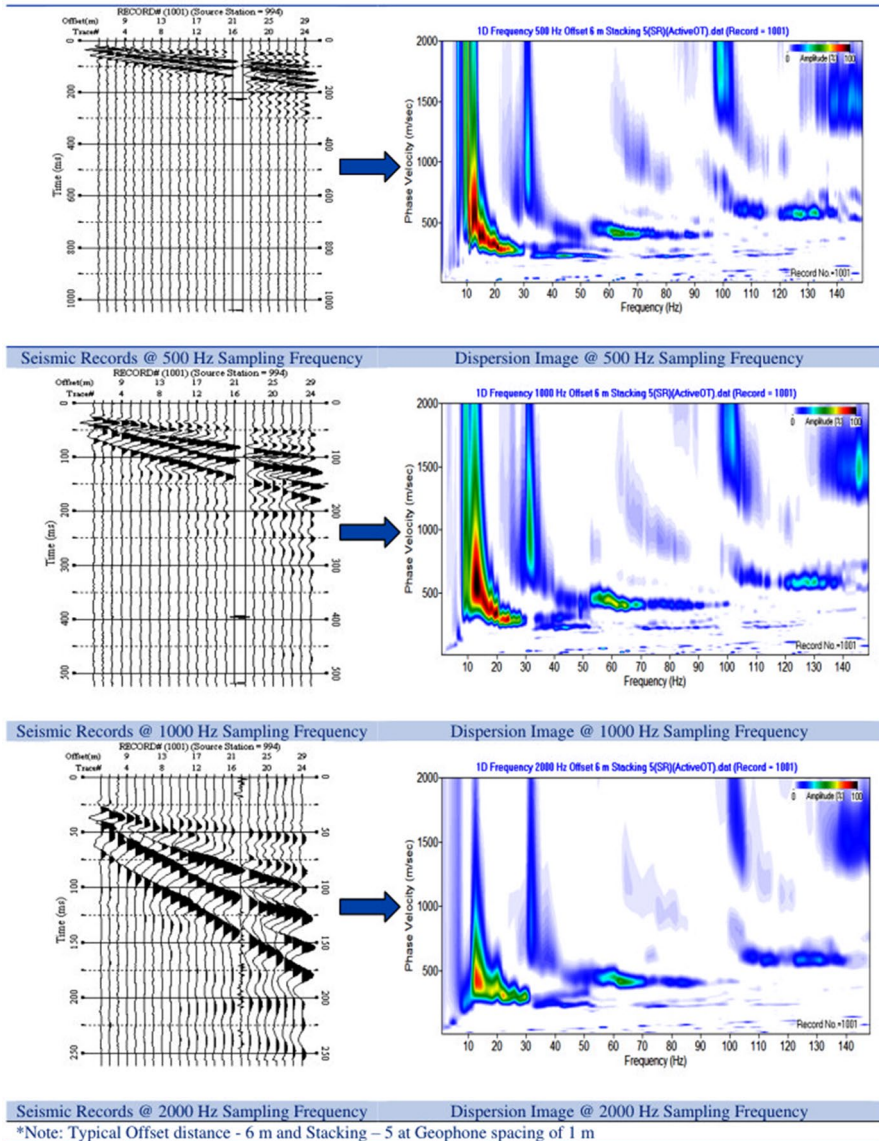


**Fig. 5** Typical seismic records and corresponding dispersion images obtained for different sampling frequencies for site MASW-4

after the active signal has fully propagated through the receiver array, resulting in a high concentration of ambient noise in the recording.

The dispersion image that corresponds to a sampling frequency of 2000 Hz is shown in Fig. 5. This image produces a low-resolution dispersion image, causes noise adulteration around the fundamental dispersion curve, and does not provide any useful information. However, the resolution of the dispersion images created with sampling frequencies of 500 Hz and 1000 Hz is acceptable; however, the resolution of the images produced with

the lower sampling frequency is superior, as evidenced by the presence of a considerable energy band until 28 Hz.

Foti et al. (2018) state that a lower sampling frequency range is advised since it can yield a high-resolution image of the dispersion analysis. The suggested range of frequencies is 500–1000 Hz. Due to the possibility of capturing a significant quantity of noise interference, choosing a high sampling frequency range for seismic wave recording (more than 2000 Hz) is not advised. The higher modes or overtone pictures caused by this interference can be seen in the dispersion curves. Because of this, the one-dimensional shear wave velocity profile that is produced may be affected in an unexpected way if the retrieved dispersion curve from the doubtful overtone image is selected in an inappropriate manner. In comparison to other frequency ranges, it was found that a sample frequency of 500 Hz delivers good dispersion image resolution, with a *SNR* of 85 percent. This discovery is based on the rationale that was provided above. This outcome is also consistent with what Park et al. (2002) has proposed in their research. In addition to this, it was found that the soil profile at the location of the study was a hard or stiff sort of medium (based on shear wave velocity profile). As shown in Fig. 5, the data's dominant frequencies and associated phase velocities range between  $V_{phmax} = 900$  m/sec and  $V_{phmin} = 280$  m/sec, with a dominating fundamental mode at approximately  $f_{min} = 11$  Hz to  $f_{max} = 28$  Hz.

According to the findings of the previous study (Park et al. 2002; Penumada and Park 2005), the following is an optimal configurational set that was discovered to have been obtained for the typical site (MASW-4): The sampling frequency is set at 500 Hz, the geophone spacing has been kept fixed as one meter, the offset distance is 6 m, and number of stacking is 5. Table 2 lists the approved data acquisition parameter as well as the optimal acquisition parameter for each of the four sites. To comprehend parameter variation and obtain an optimized outcome for a particular location, certain specifics are necessary. In order to do the inversion analysis and acquire the shear wave velocity profile, the dispersion curve was extracted for each of the four locations based on the obtained optimal array arrangement.

### 3.1.2 Appropriate selection and extraction of dispersion curve

The results of the inversion analysis are significantly influenced by the amplitude of the dispersion curve discovered in the frequency domain. The results of investigations suggest a relationship between the depth of an investigation and the amplitude of the frequencies in a band. It is commonly known that shorter wavelengths correspond to higher frequencies. Since lower wavelengths have the ability to travel further into the subsurface, higher frequencies can be used to retrieve information from greater depths. One of the reasons why shorter wavelengths are connected with higher frequencies is because of this relationship. If a lower frequency band is utilized, there is a chance that an erroneous reading will be acquired at shallow depths.

Figures 6, 7, 8 and 9 show the process of extracting the dispersion curve, which leads to the creation of the inverted profile of shear wave velocity for each of the four sites. In all possible combinations of frequency and phase velocities, the largest concentration of propagating energy is indicated by the darkest shade in the dispersion image in Figs. 6a, 7a, 8a, and 9a.

In these figures, the dispersion images are overlapped with the extracted dispersion curve (grey colored square markers), which correspond to the fundamental mode and the theoretical dispersion curve obtained in the inversion (the continuous line). Instead, the

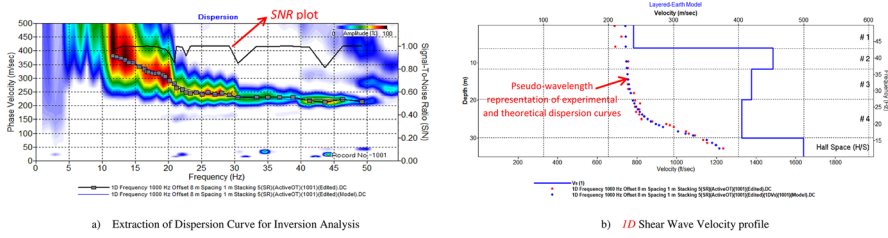


**Fig. 6** Inversion analysis of dispersion curve to produce *ID* profile of shear wave velocity at the site MASW-1

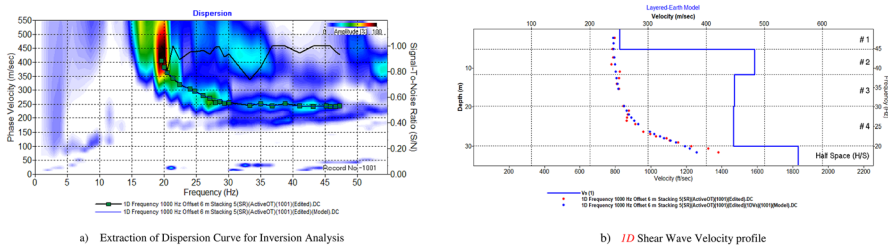


**Fig. 7** Inversion analysis of dispersion curve to produce *ID* profile of shear wave velocity at the site MASW-2

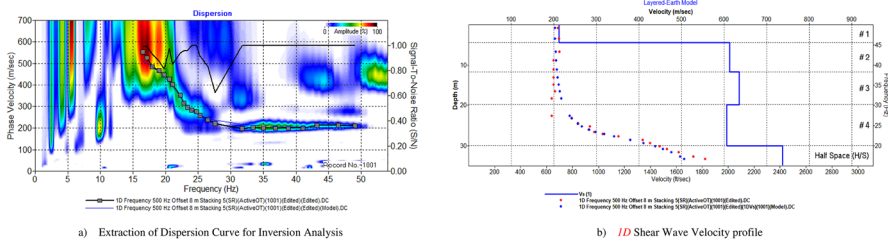


**Fig. 8** Inversion analysis of dispersion curve to produce *ID* profile of shear wave velocity at the site MASW-3

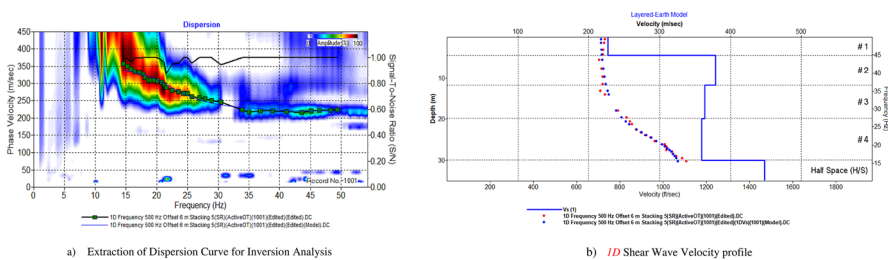


**Fig. 9** Inversion analysis of dispersion curve to produce *ID* profile of shear wave velocity at the site MASW-4

dashed line represents the  $S/N$  ratio and the color in the image indicates signal's amplitude. The fundamental mode ( $M0$  dispersion curve), are what were used to maintain the average signal-to-noise ratios of 88%, 84%, 80%, and 85% for each data point. These average  $SNR$  correspond to the plateau of the  $SNR$  plots reported in Figs. 6, 7, 8 and 9

### 3.2 Inversion analysis

The extracted dispersion curve was inverted over a wide range of frequency bands to produce the 5-layer  $I-D$  shear wave velocity ( $V_s$ ) profile, which is shown in Figs. 6b, 7b, 8b and 9b. Scatter plots colored in red and blue in the Figs. 6b, 7b, 8b and 9b correspond to the pseudo-wavelength representation (that is,  $(1.05 \div 1.1) \times VR V_s \lambda/2.5$ ) of experimental and theoretical dispersion curves. A consistent shear-wave velocity profile may be produced by the automatic selection method, which would increase the dependability of the post-processing evaluation.

Table 3 summarizes the site classification and optimal parameter for the chosen sites. This table clearly indicates that the optimal parameter, shear wave velocity, and site classification can vary based on the location of the site. When compared to the NEHRP site classification, the average shear wave velocity at 30 m depth for all the four sites were also calculated and is categorized as C and D, which falls into the category of very dense soil and soft rock and stiff soil (Refer Table 3).

The wave field data gathered in the field can be utilized to determine the shear wave velocity profile along the depth of the subsurface after being subjected to inversion analyses and dispersion curve retrieval in the third and last module of a MASW survey. This can be accomplished by using the data to determine the shear wave velocity profile along the depth of the subsurface. Because there is no straightforward method for solving the surface wave inversion problem, the process must be finished by employing an iterative or optimization method that is founded on either a deterministic, probabilistic, or mixed strategy (Lai et al. 2002; Xia et al. 2003; Lu and Zhang 2006; Song et al. 2007).

For inversion analysis, the fundamental-mode ( $M0$ ) generation algorithm (e.g., Schwab and Knopoff 1972) is most commonly used and the same is used in the present study. Although there has been a great deal of research and development in multi-mode utilization, software that takes full advantage of multi-mode while efficiently handling all the associated complications (e.g. mode misidentification and mode mix) has not yet been developed. This is because of the fact that modal identifies of higher modes in reality cannot be uniquely determined. In consequence, the higher-mode inversion methods generate results often less reliable than those from the traditional fundamental-mode ( $M0$ ) inversion method.

**Table 3**  $V_{s30}$  and site classification details of the chosen sites for Active MASW survey

Site	Coordinates	Average shear wave velocity ( $V_{s30}$ ) m/sec	Site classification as per NEHRP standards
MASW-1	22°47'46" N 86°08'42" E	364	C (Very dense soil and soft rock)
MASW-2	22°47'55" N 86°09'55" E	400	C (Very dense soil and soft rock)
MASW-3	22°46'50" N 86°10'05" E	482	C (Very dense soil and soft rock)
MASW-4	22°45'19" N 86°10'42" E	336	D (Stiff soil)

### 3.2.1 2D shear-wave velocity profile along the proposed site

Because of the nature of multichannel processing, it is usually the center location of the receiver spread to which this  $1D V_s$  profile is assigned as the most representative surface. location if the coordinate information is necessary. With accumulation of multiple number of this  $1D V_s$  profile assigned with a unique surface coordinate, a  $2D V_s$  profile is constructed by using an appropriate spatial interpolation scheme. (Table 4)

At each of the suggested locations (along the bank of the Kharkai River), an active MASW survey with a two-dimensional linear array of geophones that was moved forward by one meter between records was carried out. The configuration of this survey is shown in Fig. 10. Figures 11–14 exhibits the findings of the survey in the form of a two-dimensional variation of a shear wave velocity profile along the length of the research. These figures also include the lithology of the surrounding areas, which was collected from borehole data.

**Table 4** Detailed information of parameters for each layer

Site	Layer	Depth (m)	$V_s$ (m/s)	$V_p$ (m/s)	Poisson's ratio
MASW-1	1	6.137	239	714	0.44
	2	11.707	453	1137	0.40
	3	19.837	420	1082	0.41
	4	30.00	405	1043	0.41
	5	Half space	500	1255	0.40
MASW-2	1	5.167	251	752	0.44
	2	11.707	483	1212	0.40
	3	19.837	448	1125	0.40
	4	30.00	447	1122	0.40
	5	Half space	558	1364	0.40
MASW-3	1	4.391	212	635	0.44
	2	11.707	613	1461	0.39
	3	19.837	636	1485	0.39
	4	30.00	606	1445	0.39
	5	Half space	738	1676	0.38
MASW-4	1	4.391	227	680	0.44
	2	11.707	379	1002	0.42
	3	19.837	364	963	0.42
	4	30.00	359	951	0.42
	5	Half space	448	1125	0.41

\*Density increasing with depth in the range of 1.75 to 2.5

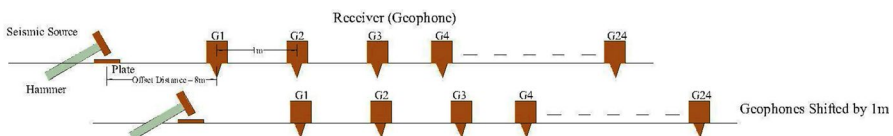


**Fig. 10** 2D arrangement of geophones shifted by 1 m after each record



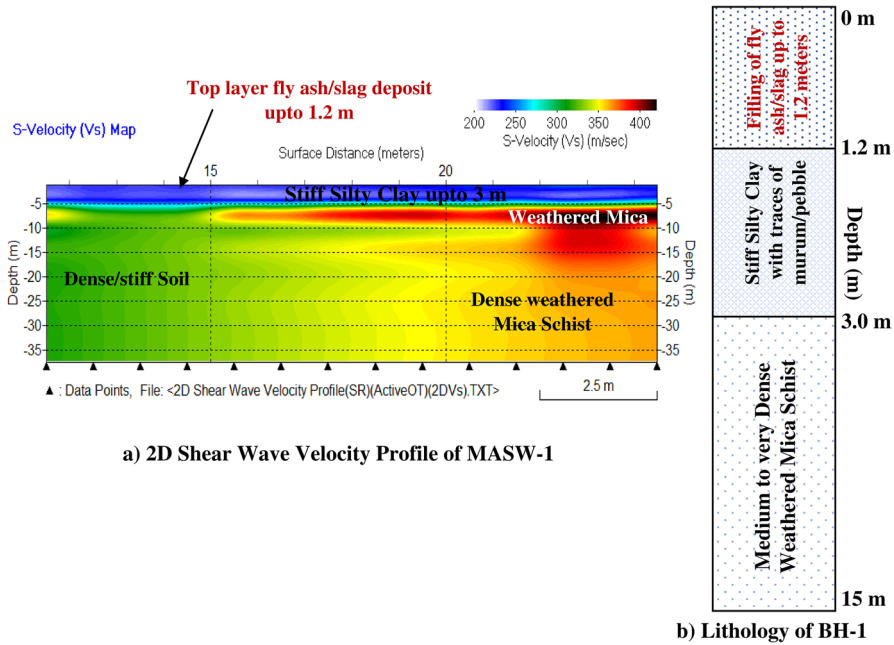


**Fig. 11** 2D Shear-Wave Velocity Profile of site MASW-1 and lithology of borehole data of site BH-1

Shear wave velocity ( $V_s$ ) profiles in two dimensions (shown in Figs. 11–14) provide information about the vertical and lateral variations of shear wave velocity ( $V_s$ ). A comparison was made between the soil profile (lithology) generated from the borehole data obtained at the location of the study and the 2D  $V_s$  profile that was obtained through MASW investigation. Figures 11–14 provide accurate information regarding the characteristics of the soil at various depths and at various distances along the surface. The borehole survey could only be completed to a depth of 10 m at three locations (MASW-2, MASW-3 & MASW-4), however information of borehole was achieved up to a depth of 15 m at site MASW-1. The existence of hard strata limited the depth to which the survey could be completed. The 1D and 2D  $V_s$  profiles that were created from the MASW survey provided information on deeper strata (up to 30 m) that could not be explored by the borehole survey.

The top layer at the proposed site (MASW-1) indicates a filling of fly ash or slag deposit up to a depth of 1.2 m, which is further followed by a layer of stiff silty clay up to 3 m depth which can also be validated from the lithology of the borehole results, obtained for nearby site BH-1, which indicates dense silty clay up to 3 m (Fig. 11). A thick layer of medium to very dense weathered mica schist ( $V_s$  beyond 400 m/s along the surface distance of 20 m from 5 m depth to below). Some traces of stiff soil have also been observed at 25 m to 35 m depth along the lateral distance on the profile.

The top layer at the proposed site (MASW-2) indicates a top layer of stiff soil with traces of pebbles, boulders, gravel, sand or murum, up to 3 m depth which is also observed in the lithology details of site BH-2 (Fig. 12). A thick layer of medium to very dense weathered mica schist ( $V_s$  beyond 400 m/s along the surface distance of 15 m from 5 m depth to below). Further at deeper depth, an increase in  $V_s$  is also observed (from 20 m depth to below). Dense/stiff soil has also been observed along the lateral distance on the profile.

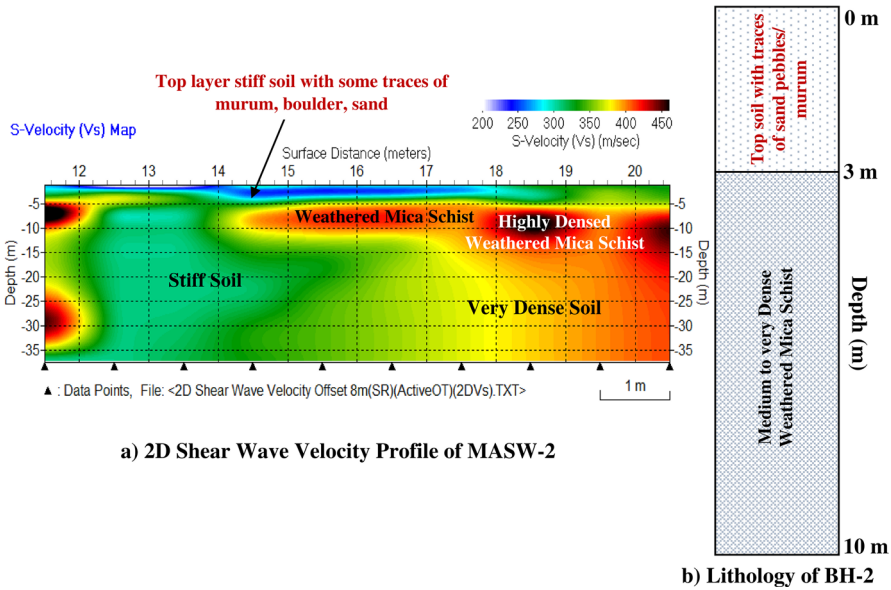


Fig. 12 2D Shear-Wave Velocity Profile of site MASW-2 and lithology of borehole data of site BH-2

The top layer at the proposed site (MASW-3) indicates a filling of iron slag deposit up to a depth of 2.3 m, which is further followed by a layer of weathered mica schist up to ~5 m depth. A thick layer of highly dense disintegrated weathered mica schist ( $V_s$  ranging 600 m/s to 1000 m/s along the surface distance of 6 m from 8 m depth to below), further the  $V_s$  increases beyond 1200 m/s (from 12 to 30 m depth) along the lateral distance of 6 to 8 m, where hard rock strata is also seen at deeper depth. This information is also supported, from the lithological details of borehole site BH-3 up to 10 m depth (Fig. 13).

The top layer at the proposed site (MASW-4) indicates a top layer of dense silty soil with traces of pebbles, boulders, gravel, sand or murum, up to a varying depth of 3 to 5 m, which is also observed in the lithology details of site BH-4 (Fig. 14). A thick layer of highly dense disintegrated weathered mica schist ( $V_s$  ranging beyond 600 m/s along the surface distance of 6 m from 7 m depth to below). Further at deeper depth, an increase in  $V_s$  is also observed (from 20 m depth to below). This information is also supported, from the lithological details of borehole site BH-4 up to 10 m depth (Fig. 14).

### 4 Conclusions

This article provides a detailed account of the Active MASW investigation that was carried out at four different suggested sites along the bank of the Kharkai River in Jamshedpur. It is necessary to conduct research at the chosen locations, which were a part of a larger study for the Jamshedpur region, in order to evaluate the underlying stratigraphy for the sake of any prospective foundation excavation and design planning. Active MASW surveys in both the first dimension (1D) and the second dimension (2D) were carried out at the location. Some noteworthy observations have been obtained as a result of the experimental investigations that have been carried out:

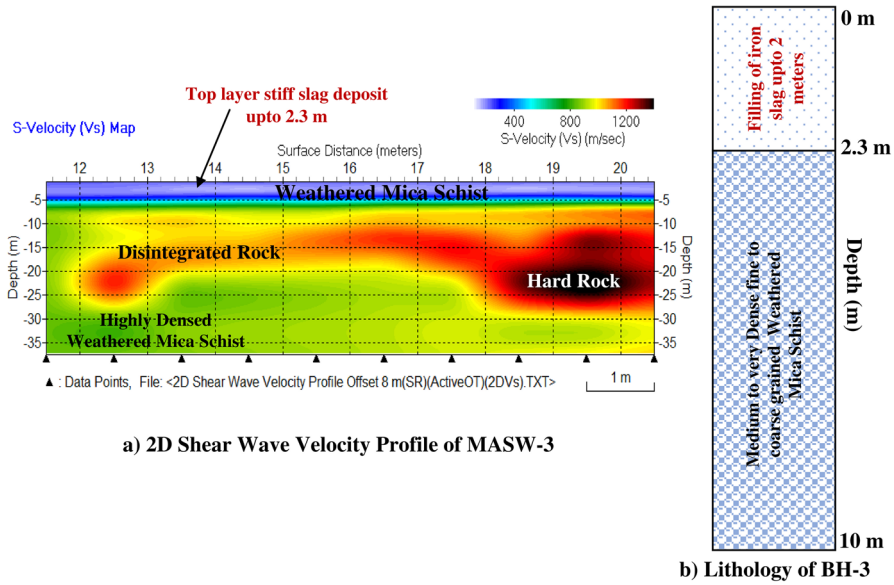


Fig. 13 2D Shear-Wave Velocity Profile of site MASW-3 and lithology of borehole data of site BH-3

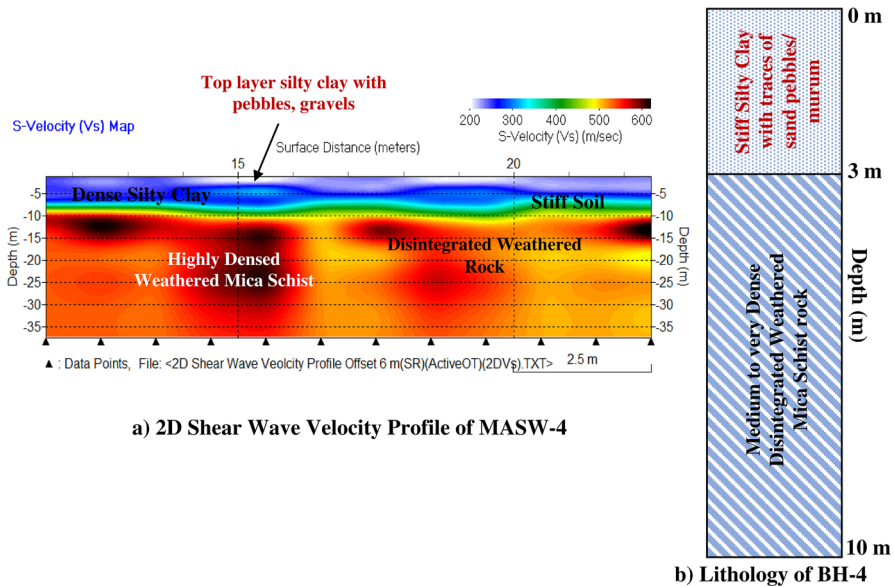


Fig. 14 2D Shear-Wave Velocity Profile of site MASW-4 and lithology of borehole data of site BH-4

- The investigations revealed that the optimal sampling frequency varies substantially depending on the conditions of the site, as was illustrated. Out of the several combinations sampling frequency and sampling time, which allows for the suitable completion of phase propagation, that value of sampling frequency is recommended. The sample time and off-

set ranges were appropriately chosen for each of the various sites in order to obtain the most accurate record possible of the wave fields that were being propagated. This was carried out in such a way that the condition of complete phase propagation across the receiver array without creating noise adulteration in the wave field record was satisfied, which led to the highest resolution dispersion image possible.

- The proposed locations were investigated in order to ascertain both the one-dimensional and the two-dimensional shear-wave velocity profiles. As recommended by the standards, a two-dimensional active MASW survey was carried out in order to determine the continuous profile of shear wave velocity across the entirety of the proposed area. The obtained profile was able to determine the presence of the stiff silty clay soil (up to a depth of 3 m), as well as the medium-to-very dense weathered mica schist (at variable locations and depths from 3 to 30 m or beyond). At site MASW-3, it has also been possible to locate hard rock strata at more profound depths. The results of the geophysical investigations were consistent with the profile that was generated from borehole measurements, or up to a depth of 10 to 15 m. Dense weathered rock was seen beyond the borehole's termination depth of 10 m, which is also shown in the MASW data beyond depths of 10–15 m. The shear-wave velocity profiles for each site exhibit excellent agreement with the information from the boreholes, demonstrating the utility of non-invasive approach for subsurface research.
- According to the geophysical investigation, the qualities of the rock layer improve as one descends deeper into the earth (that is, beyond a depth of 20 m). This indicates that strata discovered at greater depths can be recognized and offered as bearing strata.
- In general, it can be stipulated that locations in the vicinity of the Kharkai River fall into the site classification category of either C or D, which indicates a soil profile of dense soil or soft rock according to NEHRP standards.
- All of this information might serve as a foundation for any projected construction of infrastructure in the proximity area of the bank of river basin. The method that was utilized in this analysis can be applied to the design and planning of foundations for any other type of building.

**Acknowledgements** The authors warmly recognize the assistance provided by the National Institute of Technology Jamshedpur, Jamshedpur, India, in undertaking this research. Also noted is the cooperation of the Department of Civil Engineering. The Editor-in-Chief thanks the Associate Editor and the Reviewers for their constructive comments.

**Authors contribution** AI: Investigation, Methodology, Visualization, Resources, Writing—Original draft, Writing—review & editing. KKS: Conceptualization, Visualization, Writing—review & editing. VK: Conceptualization, Visualization, Writing—review & editing.

**Funding** This research did not receive any specific grant from funding agencies in the public, commercial, or not-for-profit sectors.

## Declarations

**Conflicts of interest** The authors declare that they have no known competing financial interests or personal relationships that could have appeared to influence the work reported in this paper.

## References

- Adegbola RB, Ayolabi EA, Allo W (2013) Subsurface characterization using seismic refraction and surface wave methods: a case of Lagos State University, Ojo, Lagos State. *Arab J Geosci* 6:4925–4930. <https://doi.org/10.1007/s12517-012-0784-2>
- Anbazhagan P, Sitharam TG (2008) Site characterization and site response studies using shear wave velocity. *J Seismol Earthq Eng* 10:53–67
- Anderson JG, Lee Y, Zeng Y, Day S (1996) Control of strong motion by the upper 30 meters. *Bull Seismol Soc Am* 86:1749–1759
- Ariffin J, Ismail MA, Tan C, Murtadza NM (2016) Site characterization of marine clay deposits in south seberang prai, penang using combined active and passive multichannel analysis of surface wave (MASW). *IOP Conf Ser Mater Sci Eng* 136:012032. <https://doi.org/10.1088/1757-899X/136/1/012032>
- Ashraf MAM, Kumar NS, Yusoh R, Hazreek ZAM, Aziman M (2018) Site classification using multichannel channel analysis of surface wave (MASW) method on soft and hard ground. *IOP Conf Ser J Phys Conf Ser* 995:012108. <https://doi.org/10.1088/1742-6596/995/1/012108>
- Basri K, Zainorabidin A, Talib MKA, Wahab N (2020) The optimum field configuration for active MASW survey on peat soil. *Int J Integr Eng* 12:121–130
- Borcherdt RD (1994) Estimates of site-dependent response spectra for design (methodology and justification). *Earthq Spectra* 10(4):617–653. <https://doi.org/10.1193/1.1585791>
- Dikmen U, Arisoy M, Akkaya I (2010) Offset and linear spread geometry in the MASW method. *J Geophys Eng* 7:211–222. <https://doi.org/10.1088/1742-2132/7/2/S07>
- Dobry R, Borcherdt RD, Crouse CB, Idriss IM, Joyner WB, Martin GR, Power MS, Rinne EE, Seed RB (2000) New site coefficients and site classification system used in recent building seismic code provisions. *Earthq Spectra* 16:41–67. <https://doi.org/10.1193/1.1586082>
- Eker AM, Akgün H, Kockar MK (2012) Local site characterization and seismic zonation study by utilizing active and passive surface wave methods: a case study for the northern side of Ankara, Turkey. *Eng Geol* 151:64–81. <https://doi.org/10.1016/j.enggeo.2012.09.002>
- Field E, Jacob K (1993) Monte-Carlo simulation of the theoretical site response variability at Turkey Flat, California, given the uncertainty in the geotechnically derived input parameters. *Earthq Spectra* 9:669–701
- Foti S, Hollender F, Garofalo F et al (2018) Guidelines for the good practice of surface wave analysis: a product of the InterPACIFIC project. *Bull Earthquake Eng* 16:2367–2420. <https://doi.org/10.1007/s10518-017-0206-7>
- Gabriels P, Snieder R, Nolet G (1987) In situ measurements of shear-wave velocity in sediments with higher-mode Rayleigh waves. *Geophys Prospect* 35(2):187–196
- Gosar A, Stopar R, Roser J (2008) Comparative test of active and passive multichannel analysis of surface waves (MASW) methods and microtremor HVSR method. *RMZ Mater Geoenviron* 55:41–66
- Grandjean G, Bitri A (2006) 2M-SASW: multifold multichannel seismic inversion of local dispersion of Rayleigh waves in laterally heterogeneous subsurface: application to the super-sauze earthflow, France. *Near Surf Geophys* 4:367–375. <https://doi.org/10.3997/1873-0604.2006010>
- Haloi J, Sil A (2015) Seismic site classification of a bridge site over river Barak on Silchar bypass road. *Int J Adv Earth Sci Eng* 4(1):275–282
- Imam A, Sharma KK, Kumar V, Singh N (2022) Subsurface profiling of a region in Jamshedpur city using active MASW: a case study. *Acta Geophys* 70:1601–1617. <https://doi.org/10.1007/s11600-022-00816-5>
- Kramer SL (1996) *Geotechnical earthquake engineering*. Prentice Hall, New York
- Kwok AOL, Stewart JP, Hashash YMA (2008) Nonlinear ground-response analysis of Turkey flat shallow stiff-soil site to strong ground motion. *Bull Seismol Soc Am* 98:331–343. <https://doi.org/10.1785/0120070009>
- Lai CG, Rix GJ, Foti S, Roma V (2002) Simultaneous measurement and inversion of surface wave dispersion and attenuation curves. *Soil Dyn Earthq Eng* 22:923–930. [https://doi.org/10.1016/S0267-7261\(02\)00116-1](https://doi.org/10.1016/S0267-7261(02)00116-1)
- Li J, Rosenblad B (2009) Experimental study of near-field effects in multichannel array-based surface wave velocity measurements. *Near Surf Geophys* 9:357–366
- Liu J, Xia J, Luo Y, Li X, Xu S (2004) Extracting transient Rayleigh wave and its application in detecting quality of highway roadbed. *Progress in environment. and engineering geophysics*. Proceedings of the international conference on environment and engineering geophysics (ICEEG)
- Louie JN (2001) Faster, better: shear-wave velocity to 100 meters depth from refraction microtremor arrays. *Bull Seismol Soc Am* 91:347–364. <https://doi.org/10.1785/0120000098>

- Lu L, Zhang B (2006) Inversion of Rayleigh waves using a genetic algorithm in the presence of a low-velocity layer. *Acoust Phys* 52:701–712. <https://doi.org/10.1134/S106377100606011X>
- Madun A, Supaat ME, Tajudin SA, Hazreek M, Sani S, Yusof MF (2016) Soil investigation using multichannel analysis of surface wave (MASW) and borehole. *ARPN J Eng Appl Sci* 11:3759–3763
- Miller RD, Xia J, Park CB, Ivanov JM (1999) Multichannel analysis of surface waves to map bedrock. *Lead Edge* 18:1392–1396. <https://doi.org/10.1190/1.1438226>
- Olafsdottir EA, Erlingsson S, Besson B (2016) Effects of measurement profile configuration on estimation of stiffness profiles of loose post glacial sites using MASW. In: proceedings of the 17th Nordic geotechnical meeting challenges in Nordic geotechnic (NGM 2016), Reykjavik, Iceland. Pp 327–336
- Park CB (2011) Imaging dispersion of MASW data—full Vs. selective offset scheme. *J Environ Eng Geophys* 16:13–23. <https://doi.org/10.2113/JEEG16.1.13>
- Park CB, Miller RD, Xia J (1999) Multichannel analysis of surface waves. *Geophysics* 64:800–808. <https://doi.org/10.1190/1.1444590>
- Park CB, Miller RD, Xia J, Ivanov J (2007) Multichannel analysis of surface waves (MASW)—active and passive methods. *Lead Edge* 26:01–06. <https://doi.org/10.1190/1.2431832>
- Park CB, Miller RD, Xia J (1998) Imaging dispersion curves of surface waves on multi-channel record. Proceedings of the 68<sup>th</sup> annual international meeting of society of exploration geophysics. Expanded abstract. 1377–1380. <https://doi.org/10.1190/1.1820161>
- Park CB, Miller RD, Xia J (2001) Offset and resolution of dispersion curve in multichannel analysis of surface waves (MASW). In: 14th EEGS symposium on the application of geophysics to engineering and environmental problems, pp 1–6. [https://doi.org/10.3997/2214-4609-PDB.192.SSM\\_4](https://doi.org/10.3997/2214-4609-PDB.192.SSM_4)
- Park CB, Miller RD, Miura H (2002) Optimum field parameters of an MASW survey. Japanese society of exploration geophysics (SEG-J), Extended abstracts. Pp 1–6
- Pegah E, Liu H (2016) Application of near-surface seismic refraction tomography and multichannel analysis of surface waves for geotechnical site characterizations: a case study. *Eng Geol* 208:100–113. <https://doi.org/10.1016/j.enggeo.2016.04.021>
- Penumadu D, Park CB (2005) Multichannel analysis of surface wave (MASW) method for geotechnical site characterization. Geo-frontiers congress. Texas, United State
- Rahimi S, WoodTeague CM (2021) Performance of different transformation techniques for MASW data processing considering various site conditions, near-field effects, and modal separation. *Surv Geophys* 42:1197–1225
- Rahimi S, Wood CM, Himel AK (2022) Practical guidelines for near-field mitigation on array-based active surface wave testing. *Geophys J Int* 229(3):1531–1549. <https://doi.org/10.1093/gji/ggac011>
- Rathje EM, Kottke AR, Trent WL (2010) Influence of input motion and site property variabilities on seismic site response analysis. *J Geotech Geoenviron Eng* 136(4):607–619. [https://doi.org/10.1061/\(ASCE\)GT.1943-5606.0000255](https://doi.org/10.1061/(ASCE)GT.1943-5606.0000255)
- Salas-Romero S, Malehmir A, Snowball I, Brodic B (2021) Geotechnical site characterization using multichannel analysis of surface waves: a case study of an area prone to quick-clay landslides in southwest Sweden. *Near Surf Geophys* 19:699–715. <https://doi.org/10.1002/nsg.12173>
- Sanchez-Salinero, Roesset, Shao, Stokoe II, Rix (1987) Analytical evaluation of variables affecting surface wave testing of pavements. In: Transportation research record
- Schwab FA, Knopoff L (1972) Fast surface wave and free mode computations. *Methods Comput Phys Adv Res Appl* 11:87–180. <https://doi.org/10.1016/B978-0-12-460811-5.50008-8>
- Socco LV, Boiero D, Foti S, Wisen R (2009) Laterally constrained inversion of ground roll from seismic reflection records. *Geophysics* 74:35–45. <https://doi.org/10.1190/1.3223636>
- Socco LV, Strobbia C (2004) Surface-wave method for near-surface characterization: a tutorial. *Near Surf Geophys*. <https://doi.org/10.3997/1873-0604.2004015>
- Socco LV, Foti S, Boiero D (2010) Surface-wave analysis for building near-surface velocity models—Established approaches and new perspectives. *Geophysics* 75:75A83–75A102
- Song X, Gu H, Liu J, Zhang X (2007) Estimation of shallow subsurface shear-wave velocity by inverting fundamental and higher-mode Rayleigh waves. *Soil Dyn Earthq Eng* 27:599–607. <https://doi.org/10.1016/j.soildyn.2006.12.003>
- Stewart, Afshari, Hashash (2014) Guidelines for performing hazard-consistent one dimensional ground response analysis for ground motion prediction. In: PEER report 2014. Berkeley: University of California
- Stokoe II KH, Hwang S, Joh SH (2017) Spectral-analysis-of-surface-waves (SASW) testing to evaluate vs profiles at geotechnical and geological site. 16th world conference on earthquake engineering, 16WCEE 2017, Santiago Chile. [https://sut-us.org/pages\\_data/files/Paper-3\\_637257398819967200.pdf](https://sut-us.org/pages_data/files/Paper-3_637257398819967200.pdf)

- Strobbia F (2006) Multi-offset phase analysis of surface wave data (MOPA). *J Appl Geophys* 59:300–313
- Thitimakorn T (2013) Development of a NEHRP site classification map of Chiang Mai city, Thailand, based on shear-wave velocity using the MASW technique. *J Geophys Eng* 10:45007. <https://doi.org/10.1088/1742-2132/10/4/045007>
- Tian G, Steeples DW, Xia J, Miller RD, Spikes KT, Ralston MD (2003a) Multichannel analysis of surface wave method with the autojuggie. *Soil Dyn Earthq Eng* 23:243–247. [https://doi.org/10.1016/S0267-7261\(02\)00214-2](https://doi.org/10.1016/S0267-7261(02)00214-2)
- Tian G, Steeples DW, Xia J, Spikes KT (2003b) Useful resorting in surface wave method with the autojuggie. *Geophysics* 68:1906–1908. <https://doi.org/10.1190/1.1635043>
- Tokimatsu (1995) Geotechnical site characterization using surface waves. In: 1st international conference on earthquake geotechnical engineering. Tokyo, Japan: Balkema, pp 1333–1368
- Trupti S, Srinivas KNSSS, Kishore PP, Seshunarayana T (2012) Site characterization studies along coastal Andhra Pradesh-India using multichannel analysis of surface waves. *J Appl Geophys* 79:82–89. <https://doi.org/10.1016/j.jappgeo.2011.12.006>
- Xia J, Miller RD, Park CB (1999) Estimation of near-surface shear-wave velocity by inversion of Rayleigh waves. *Geophysics* 64:691–700. <https://doi.org/10.1190/1.1444578>
- Xia J, Miller RD, Park CB, Tian G (2003) Inversion of high frequency surface waves with fundamental and higher modes. *J Appl Geophys* 52:45–57. [https://doi.org/10.1016/S0926-9851\(02\)00239-2](https://doi.org/10.1016/S0926-9851(02)00239-2)
- Xia J, Miller RD, Park CB, Ivanov J (2004) Utilization of high-frequency Rayleigh waves in near-surface geophysics. *Lead Edge* 23:753–759. <https://doi.org/10.1190/1.1786895>
- Yoon S, Rix GJ (2009) Near-field effects on array-based surface wave methods with active sources. *J Geotech Geoenviron Eng*. [https://doi.org/10.1061/\(ASCE\)1090-0241\(2009\)135:3\(399\)](https://doi.org/10.1061/(ASCE)1090-0241(2009)135:3(399))
- Zywicki R (2005) Mitigation of near-field effects for seismic surface wave velocity estimation with cylindrical beamformers. *J Geotech Geoenviron Eng* 131:970–977

Springer Nature or its licensor (e.g. a society or other partner) holds exclusive rights to this article under a publishing agreement with the author(s) or other rightsholder(s); author self-archiving of the accepted manuscript version of this article is solely governed by the terms of such publishing agreement and applicable law.